Fast Evaluation of Geometries and Properties of Excited Molecules in Solution: A Tamm-Dancoff Model with Application to 4-Dimethylaminobenzonitrile

Roberto Cammi,[‡] Benedetta Mennucci,[†] and Jacopo Tomasi*[,†]

Dipartimento di Chimica Generale ed Inorganica, Università di Parma, viale delle Scienze, 43100 Parma, Italy, and Dipartimento di Chimica e Chimica Industriale, Università di Pisa, via Risorgimento 35, 56126 Pisa, Italy

Received: January 11, 2000; In Final Form: March 23, 2000

We present a method to evaluate ab initio energy, wave function, and gradient of a solvated molecule in an electronically excited state. In particular, this paper extends the Polarizable Continuum Model (PCM) to a specific level of theory for the interpretation of the electronic spectra: configuration interaction (CI) among all singly substituted determinants using a Hartree−Fock reference state. This method, in very wide use, allows investigations of both structures and properties of electronically excited molecules through the evaluation of analytical energy derivatives with respect to various parameters. The most relevant formal aspects on the extension of the theory to solvated systems are discussed, and numerical applications to the study of geometries and one-electron properties of the low-lying excited states of 4-dimethylamino benzonitrile (DMABN) in acetonitrile solution are presented.

1. Introduction

This paper presents a theoretical formulation and the related computational implementation of analytical gradients for molecular solutes in excited electronic states.

The method is formulated within the framework of a solvent continuous model, and it belongs to the set of ab initio approaches of medium computational cost, namely, the configuration interaction (CI) among all singly substituted determinants using a Hartree−Fock reference state. This method, which can be seen as a specific case of the more general random phase approximation (RPA), has been widely used in the past under several names: single excitation configuration interaction (SECI), monoexcited configuration interaction, the Tamm-Dancoff approximation (TDA) or, to connect it with other CI terminology, CI-singles (CIS). In the following, we shall adopt the TDA. This is the simplest level of theory that can be used to include some of the effects of electron correlation via the mixing of excited determinants, and until now, it has shown very reliable performances in the evaluation of properties through the use of analytic gradients.[1] Examples of TDA studies of potential energy surfaces of excited states are numerous in the literature concerning isolated systems, whereas much less has been done for condensed phases.

When solvent effects are included in methods devoted to the study of excited states, some additional aspects not present in isolated systems have to be considered. The transition to electronically excited states, in fact, always involves a dynamical process in which solvent relaxation times cannot be neglected. This aspect has been discussed many times in the past,[2] and it is not worth repeating it now; we only state that both equilibrium and nonequilibrium solute−solvent descriptions may play a role. Some further comments will be given in the following sections. Another important aspect to consider is the formal definition of the energies of the excited states in solution. Generally, the energetic quantity used to describe solvated systems has the status of a free energy.

The TDA method, here treated as limit case of RPA, defines as excitation energies the poles of the linear response function, for which the status of free energy is not evident. However, the good results obtained until now using these poles and the related residues in the calculation of molecular properties of solutes in continuum dielectrics[3,4] seem to confirm their numerical reliability and, from an empirical point of view, to show that they represent a good approximation of the exact free energies for excited states of molecular solutes.

The linear response theory for solvated systems treated within the Polarizable Continuum Model (PCM)[5] in its revised version known as Integral Equation Formalism (IEF)[6] has been presented in ref 3. Here, it will be reconsidered in the approximated TDA method and applied to the evaluation of analytical gradients. The reader is referred to ref 3 for a detailed analysis of all the formal aspects of the general theory.

The application of response theories to the calculation of energy gradients for excited states is well-known;[7] however, it has recently acquired a new and important role when linked to density functional theory (DFT). In the latter case, in fact, the response methods become the fundamental tool to study excited states. Some important developments in this direction have been already presented for isolated molecules,[8−13] but have not yet been extended to solvated systems. The formulation we present here for analytical gradients within the conventional TDA, but immediately extensible to the more complete RPA scheme, can be thus seen as the theoretical basis to be generalized to time-dependent density functional theory (TD-DFT).

In section 2, we present the PCM-TDA formalism for both energy and gradients, and in section 3, we report a numeric application to the study of geometries and properties of ground and singlet excited states of 4-(*N*,*N*-dimethylamino)benzonitrile (DMABN) in vacuo and in acetonitrile solution. The analysis on excited-state energies is also supported by single-point TDDFT calculations.

* Corresponding author. E-mail: tomasi@dcci.unipi.it.
[†] Università di Pisa.
[‡] Università di Parma.

10.1021/jp000156l CCC: $19.00
Published on Web 05/17/2000

2. Energy Derivatives for Excited States in the PCM-TDA

2.1. Excited-State Energies. From the linear response theory within the RPA scheme, the excitation energies can be obtained as a solution of the generalized eigenvalue problem:

$$\begin{pmatrix} \tilde{\mathbf{M}} & \tilde{\mathbf{N}} \\ \tilde{\mathbf{N}} & \tilde{\mathbf{M}} \end{pmatrix} \begin{pmatrix} \mathbf{X}_p \\ \mathbf{Y}_p \end{pmatrix} = \omega_p \begin{pmatrix} \mathbf{1} & \mathbf{0} \\ \mathbf{0} & -\mathbf{1} \end{pmatrix} \begin{pmatrix} \mathbf{X}_p \\ \mathbf{Y}_p \end{pmatrix} \tag{1}$$

where $\mathbf{X}_p$ and $\mathbf{Y}_p$ are the RPA amplitude vectors.[14]

The matrixes $\tilde{\mathbf{M}}$ and $\tilde{\mathbf{N}}$ for a PCM solvated system are (see ref 3)

$$\tilde{M}_{ai,bj} = \delta_{ai,bj}(\epsilon_a - \epsilon_i) + \langle aj||ib\rangle + B_{ai,bj} \tag{2}$$

$$\tilde{N}_{ai,bj} = \langle ab||ij\rangle + B_{ai,bj} \tag{3}$$

where $\mathbf{X}_p$ and $\mathbf{Y}_p$ are antisymmetrized two-electron repulsion integrals over the molecular spin-orbitals $\{|p\rangle\}$ with orbital energies $\{\epsilon_p\}$. Spin−orbitals are here denoted according to the usual convention: *a*, *b*... if virtual (v), *i*, *j*... if occupied (o), and *p*, *q*... when referring to general molecular orbitals.

Concerning the solvent-induced integrals $B_{ai,bj}$ appearing in eqs 2−3, we prefer to postpone any comment to the following section; here, we only recall that they can be described as the interaction between the solute transition charge density associated with the MO's $|a\rangle$ and $|i\rangle$ and the response of the solvent induced by the parallel charge density due to the MO's $|b\rangle$ and $|j\rangle$.

In the limit of singly excited configuration interaction only (i.e., in the TDA scheme), $\tilde{\mathbf{N}}$ matrix elements disappear, and eq 1 reduces to a simpler Hermitian eigenvalue problem of the form

$$\tilde{\mathbf{M}}\mathbf{X}_p = \omega_p \mathbf{X}_p \tag{4}$$

In this framework, the excitation energy ω_p becomes

$$\omega_p = \sum_{ai}(\epsilon_a - \epsilon_i)X_{ai}^2 + \sum_{abij}[\langle ib||aj\rangle + B_{ai,bj}]X_{ai}X_{bj} \tag{5}$$

where now X_{ai} can be associated with the CI-singles coefficients.

Within the assumption commented on in the Introduction on the meaning of excitation energies for solvated systems, the total energy for a TDA excited-state *p* in the presence of solvent effects becomes

$$G_p^{\mathrm{TDA}} = G_{gs}^{\mathrm{HF}} + \omega_p \tag{6}$$

where G^{HF} is the free energy of the HF ground state and ω_p is the TDA excitation energy.

2.2. Analytical Gradients. By direct differentiation of eq 5 with respect to a parameter *x*, we obtain the derivative of the PCM-TDA excitation energies (from now on we skip the subscript *p* indicating the specific electronic state):[1]

$$\omega^x = \sum_{ai}(\epsilon_a^x - \epsilon_i^x)X_{ai}^2 + \sum_{ijab}\tilde{M}'^x_{ai,bj}X_{ai}X_{bj} \tag{7}$$

where we have assumed all real quantities, and $\tilde{\mathbf{M}}'$ indicates the solvent-modified two-electron integral derivatives, that is,

$$\tilde{M}'^x_{ai,bj} = \langle ib||aj\rangle^x + B^x_{ai,bj} \tag{8}$$

Equation 7 can be further developed by exploiting the derivative of the spin-orbitals and of the corresponding orbital energies in the framework of the "Coupled Perturbed Hartree−Fock Theory" (CPHF) for solvated systems.

The derivatives of the molecular orbitals (MOs) required in eq 8 will contain two types of terms: those arising from the changes in the AO basis functions and those from the changes in the MO coefficients. The latter can be expressed in terms of the CPHF coefficients U_{pq}^x. The elements of the unknown matrix $\mathbf{U}^x$ can be obtained from the following equation:

$$U_{ai}^x = \sum_{bj}(\tilde{A}^{-1})_{ai,bj}\frac{\tilde{Q}_{bj}^x}{\epsilon_j - \epsilon_b} \tag{9}$$

In the following discussion we shall show that all terms of eq 9 are modified by the presence of the solvent.

In the PCM framework, the solvent contributions, here limited to a purely electrostatic description, can be translated into a form recalling the vacuum system by defining one- and two-electron terms, indicated as $\mathbf{j}^R$ and $\mathbf{X}^R$, respectively. In brief, the solvent response to the presence of the electric field generated by the solute charge distribution (assumed to be contained in a volume of known form and dimension, the molecular cavity) is represented in terms of an apparent charge spread on the cavity surface. This charge is discretized into point charges $\mathbf{q}$ by partitioning the cavity surface into patches of known area (the tesserae). Finally, if we distinguish the two sources of the solute's field, namely, the solute's nuclei and electrons, the apparent point charges, $\mathbf{q}$, can be divided into two separate sets defined as electrons and nuclei-induced charges. In this scheme, the definitions of the two solvent-induced terms when expanded on the AO basis set become

$$j_{\mu\nu}^R = -\sum_k V_{\mu\nu}(s_k)q^N(s_k) \tag{10}$$

$$X_{\mu\nu}^R = -\sum_k V_{\mu\nu}(s_k)q^{\mathrm{e}}(s_k;\mathbf{P}^{\mathrm{HF}}) = \sum_{\lambda\sigma}P_{\lambda\sigma}^{\mathrm{HF}}B_{\mu\nu,\lambda\sigma} \tag{11}$$

where matrix $\mathbf{V}$ contains the solute's AO potential integrals computed on the cavity tesserae, that is, at the positions s_k of the apparent charges. The dependence of the electron-induced charges, $\mathbf{q}^{\mathrm{e}}$ on the one-electron density matrix (here, the HF density $\mathbf{P}^{\mathrm{HF}}$) has been exploited to rewrite $\mathbf{X}^R$ in terms of the previously introduced solvent-induced integrals $B_{ai,bj}$ (here transformed in the AO basis). In fact, introducing into eq 11 the analytical expression giving the PCM-IEF apparent charges, namely,

$$q^{\mathrm{e}}(s_k;\mathbf{P}^{\mathrm{HF}}) = \sum_{\lambda\sigma}\mathbf{P}_{\lambda\sigma}^{\mathrm{HF}}\sum_l C_{kl}^{-1}V_{\lambda\sigma}(s_l) \tag{12}$$

where the $\mathbf{C}$ matrix is defined in terms of parameters depending on the cavity geometry and the solvent permittivity,[6] the solvent-induced integrals reduce to

$$B_{\mu\nu,\lambda\sigma} = -\sum_{kl}V_{\mu\nu}(s_k)C_{kl}^{-1}V_{\lambda\sigma}(s_l) \tag{13}$$

This representation allows one to redefine both $\tilde{\mathbf{A}}$ and $\tilde{\mathbf{Q}}^x$ matrixes of the basic CPHF eq 9 as follows:[16]

$$\tilde{A}_{ai,bj} = \delta_{ab}\delta_{ij} + \frac{\langle ab||ij\rangle + \langle aj||ib\rangle + 2B_{ai,bj}}{\epsilon_a - \epsilon_i} \tag{14}$$

$$\tilde{Q}^x_{pq} = [h^x_{pq} + j^{R,x}_{pq}] - S^x_{pq}\epsilon_q - \sum_{kl} S^x_{kl}[\langle pl||qk\rangle + B_{pq,kl}] + \sum_{\mu\nu\lambda\sigma} (c_{\mu p})^* c_{\nu q} P_{\lambda\sigma}[\langle \mu\lambda||\nu\sigma\rangle^x + B^x_{\mu\lambda,\nu\sigma}] \quad (15)$$

In the same way, the general expression for orbital energy derivatives becomes

$$\epsilon^x_p = \tilde{Q}^x_{pp} + \sum_{gm} U^x_{gm}(\langle pm||pg\rangle + \langle pg||pm\rangle + 2B_{gm,pp}) \quad (16)$$

By introducing eqs 9−16 into eq 7, we can rewrite the derivative of the PCM-TDA eigenvalues as sum of two contributions:

$$\omega^x = \omega^x(\mathrm{MO}) + \omega^x(\mathrm{AO}) \quad (17)$$

where ω^x(MO) collects all terms containing CPHF coefficients $U^x{}_{ai}$ and ω^x(AO) collects those related to the derivatives of the basis functions and of the unperturbed MO coefficients.

The presence of U^x_{ai} should imply solving as many PCM-CPHF equations as the perturbative parameters (for example, one for each geometric degree of freedom in a geometry optimization). However, by exploiting the Z-vector method[17] it is possible to reduce the problem to a single CPHF equation that is independent of the perturbation:

$$\sum_{bj} P^\Delta_{bj}(\epsilon_j - \epsilon_b)\tilde{A}_{bj,ai} = \tilde{L}_{ai} \quad (18)$$

where P^Δ_{bj} is the (v−o) block of the relaxed density matrix and the elements of the solvent-including Lagrangian[16] are given by

$$\tilde{L}_{gm} = J_{gm} + \sum_{ij} P^\Delta_{ij}\tilde{M}'_{ij,mg} + \sum_{ab} P^\Delta_{ab}\tilde{M}'_{ab,mg} \quad (19)$$

with

$$J_{gm} = 2\sum_{iab} X_{bm}X_{ai}\tilde{M}'_{bg,ai} - 2\sum_{ija} X_{ai}X_{gm}\tilde{M}'_{jm,ai} \quad (20)$$

Equations 18−20 show that solvent effects are taken in full account also in the evaluation of the excited-state density matrix and, as a consequence, in the orbital relaxation following the initial charge rearrangement due to excitation. As we shall show in the next numerical section, it is the use of this true TDA density matrix that allows a reliable computation of one-electron properties of the excited state for solvated molecules.

In this scheme, ω^x(MO) becomes (in the AO basis):

$$\omega^x(\mathrm{MO}) = \sum_{\mu\nu} P^\Delta_{\mu\nu}(h^x_{\mu\nu} + j^x_{\mu\nu}) + \sum_{\mu\nu} W^\Delta_{\mu\nu}S^x_{\mu\nu} \quad (21)$$

where the AO transformed matrixes of the relaxed density $\mathbf{P}^\Delta$ and the energy weighted density $\mathbf{W}^\Delta$ are obtained by transforming the entire MO basis Δ matrix

$$R^\Delta_{\mu\nu} = \sum_{pq} (c_{\mu p})^* c_{\nu q} R^\Delta_{pq} \quad (22)$$

For $\mathbf{P}^\Delta$ we have then to consider

$$P^\Delta_{ij} = -\sum_a X_{ai}X_{aj} \quad (23)$$

$$P^\Delta_{ab} = -\sum_i X_{ai}X_{bi} \quad (24)$$

whereas for $\mathbf{W}^\Delta$ we can define

$$W^\Delta_{ij} = -\sum_{nab} X_{ai}X_{bn}\tilde{M}'_{aj,bn} - P^\Delta_{ij}\epsilon_i - \sum_{pq} P^\Delta_{pq}\tilde{M}'_{ij,pq} \quad (25)$$

$$W^\Delta_{ab} = -\sum_{ijf} X_{ai}X_{fj}\tilde{M}'_{bi,fj} - P^\Delta_{ab}\epsilon_a \quad (26)$$

$$W^\Delta_{ai} = 2\sum_{iab} X_{bm}X_{ai}\tilde{M}'_{bg,ai} - P^\Delta_{ai}\epsilon_i \quad (27)$$

The contribution ω^x(AO) of eq 17 can be rewritten converting the indices in the AO basis as

$$\omega^x(\mathrm{AO}) = \sum_{\mu\nu\lambda\sigma}[(X_{\mu\nu}X_{\lambda\sigma} - X_{\mu\sigma}X_{\lambda\nu})\langle\mu\lambda|\nu\sigma\rangle^x + X_{\mu\nu}X_{\lambda\sigma}B^x_{\mu\nu,\lambda\sigma}] \quad (28)$$

where

$$X_{\mu\nu} = \sum_{pq}(c_{\mu a})^* c_{\nu i}X_{ai} \quad (29)$$

Introducing eqs 21 and 28 into eq 17, we obtain the final expression for the derivative of the PCM-TDA eigenvalues as

$$\omega^x = \sum_{\mu\nu} P^\Delta_{\mu\nu}(h^x_{\mu\nu} + j^{R,x}_{\mu\nu}) + \sum_{\mu\nu} W^\Delta_{\mu\nu}S^x_{\mu\nu} + \sum_{\mu\nu\lambda\sigma}[(X_{\mu\nu}X_{\lambda\sigma} - X_{\mu\sigma}X_{\lambda\nu})\langle\mu\lambda|\nu\sigma\rangle^x + X_{\mu\nu}X_{\lambda\sigma}B^x{}_{\mu\nu,\lambda\sigma}] \quad (30)$$

Equation 30 can be finally summed to the standard HF contribution to give the expression for the total free energy gradient of each state p in the presence of the solvent:

$$G^{\mathrm{TDA},x}_p = G^{\mathrm{HF},x}_{gs} + \omega^x_p \quad (31)$$

For the description of the HF gradient contribution $G^{\mathrm{HF},x}_{gs}$, the reader is referred to the original papers[18] on the recently developed formulation to get efficient analytical free energy gradients within the PCM-IEF scheme.

It is worth noting that eqs 30−31 represent the generalization of the TDA energy gradients to solvated systems; to get a more direct comparison with the gas-phase analog, we refer to the original paper by Foresman et al.[1] We also observe that the solvent-induced terms appearing in eq 30 can be straightforwardly shifted to the parallel expressions for the RPA scheme[3] and for the TDDFT approach.[13]

3. Examples of Calculations

In this section, we present some preliminary results on an articulate study we are performing on the ground and singlet excited states of 4-(*N*,*N*-dimethylamino)-benzonitrile (DMABN) both in vacuo and in solution. Here, the attention will be mainly focused on the evaluation of optimized geometries for the lowest excited states, applying the TDA-derivative procedure presented in the previous section. In a forthcoming paper[19] such geometries will be exploited to get accurate excitation energies (both of absorption and fluorescence) and related transition quantities through more extended quantum mechanical calculations. DMABN is the prototype of a group of organic donor−acceptor compounds that exhibit dual fluorescence in polar solvent.[20] In addition to the normal fluorescence band (L_b-type) observed in vacuo (and in apolar solvents) that has been assigned to a moderately polar locally excited state (LE), a second "anomalous" band (L_a-type) arises in polar solvents.

This phenomenon has generally been attributed to an intramolecular charge−transfer (ICT) process in the electronically

excited singlet state leading to a highly polar CT state.[21] At present, the "twisted" ICT (TICT) concept is the most commonly accepted: the charge separation is believed to be combined with a rotation (the twisting) of the amino group from the parallel to the perpendicular position with respect to the benzene ring, leading to a decoupling of the amino and benzene parts of the molecule. Other models involving further motions in the molecule (for example, a wagging of the donating amino nitrogen[22]) have been proposed, but the existing calculations largely support the TICT model.[23]

All the proposed models, even if introducing different descriptions of the phenomenon, agree on a basic point largely confirmed by experiments, namely, that the interaction with a polar solvent is necessary to stabilize the CT fluorescing state. Despite this well-established feature, the validity of the investigations on solvent effects is still rather limited, most being based on semiempirical methods[24] or limited to the use of nonoptimized geometries.[25] The following results concerning the study of geometries of the ground and singlet excited states of DMABN when immersed in acetonitrile solution represent one of the first examples of accurate ab initio calculations in the presence of solvent effects.

Ground-state optimizations were performed at the density functional (DFT) level of theory with the hybrid functional B3LYP and the 6-31G(d) basis set. The same functional and basis set were also used to perform single-point calculations at the TDDFT level. Optimizations in the electronically excited states were obtained with the same basis set by applying the PCM-TDA method we presented in the previous section. All calculations were performed on a development version of the Gaussian program package.[26] Regarding the choice of the basis set, one could argue that the limited 6-31G(d) is inadequate to properly describe excited states; however, previous calculations[27] on the same system and with the same level of theory show that the results indeed depend very little on the quality of the basis set and that even when discarding all polarization and diffuse functions, one obtains sufficiently accurate results. In addition, the main interest here is the study of geometry changes and not the evaluation of very accurate excitation energies; we are thus sufficiently confident on the validity of the chosen basis set.

The numerical values of the solvent-dependent quantities that need to be defined concerns cavity parameters and dielectric constants. As said previously, the solute is embedded in a molecular cavity, here obtained in terms of interlocking spheres centered on the heavy nuclei of each group, namely, 6 carbons in the benzene ring, C and N in the nitrile, and N and two carbons in the dimethylamino group. The chosen radii are 1.9 for the four standard (i.e., bonded to an hydrogen atom) aromatic carbons and 1.7 for both the other two carbon atoms of the ring and for the nitrile carbon, 2.0 for the two methyl carbons, and 1.6 for both the nitrile and the amino N. All the radii were then multiplied by 1.2 in order to take into account the impenetrating core of the solvent molecules. Finally, a value of 36.64 for the static dielectric constant was used to represent the acetonitrile solvent.

We recall that all data presented below about excited states were obtained assuming a complete relaxation of the solvent with respect to changes in the solute charge distribution due to excitation processes. In the Introduction, we mentioned the importance of possible nonequilibrium interactions between solute and solvent; the times usually involved in electronic transitions in fact can be so short that a large part of the solvent response does not manage to immediately follow the fast changes but remains frozen to the previous condition of equilibrium.[28] Here, however, the phenomena we consider (geometry optimizations and static properties) can be reliably assumed to involve times long enough to allow a complete relaxation of the solvent, which can always completely equilibrate with the excited solute.

TABLE 1: B3LYP/6-31G(d) Optimized Geometries for the Ground State of DMABN Both In Vacuo and in Acetonitrile Solution[a]

	vacuum	acn	exp
$R_{N_8C_7}$	1.1647	1.1668	1.145
$R_{C_7C_1}$	1.4290	1.4237	1.427
$R_{C_1C_2}$	1.4057	1.4093	1.388
$R_{C_2C_3}$	1.3854	1.3834	1.370
$R_{C_3C_4}$	1.4178	1.4228	1.400
$R_{C_4N_9}$	1.3768	1.3684	1.365
$R_{N_9C_{10}}$	1.4542	1.4589	1.456
$\angle C_2C_1C_7$	120.8	120.7	120.9
$\angle C_3C_4N_9$	121.3	121.3	–
$\angle C_{10}N_9C_{11}$	119.7	119.4	116.4

[a] Atom labels are reported in the text. Bond lengths are in Å, and angles are in degrees.

As a last preliminary note, we underline that the stability of the reported optimized structures has not been further checked by calculating the Hessian matrix; the extension of PCM-TDA to the evaluation of analytical second derivatives in fact still in progress.

Below, we report the atom labeling used in the following tables and in the analysis of the results.

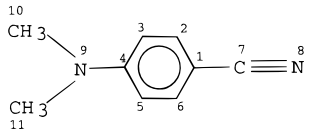

In Table 1, a selection of optimized geometrical parameters for the ground state of DMABN both in vacuo and in solution is reported; in both cases, a planar structure is obtained. The data of Table 1 show the stiffness characterizing this molecule, whose geometry changes very little in passing from vacuum to acetonitrile solution. Concerning the isolated system, the computed geometries are similar to previous calculations obtained at the HF and MP2 level of theory[29] (once again, the largest discrepancies are found for the nitrile bond length) as well as to the experimental data from crystallographic measurements.[30] We recall that in the crystal structure, the system is no longer planar; however, a wagging angle of 12° is observed, where we define as wagging angle the angle between the planes spanned by $C_{10}-C_{11}-N_9$ and $C_4-C_2-C_6$.

In Table 2, we report the same set of data as obtained by optimizing the structure of the lowest singlet excited state of DMABN in acetonitrile in both planar and twisted structures (we indicated as twisted the structure obtained with a 90° rotation of the amino group with respect to the benzene ring). Since no experimental data are available, for comparison we report the same values obtained for the twisted structure in vacuo; in Table 2, no data are given for the planar case in vacuo, as in this case the different nature of the excited state prevents a correct comparison. More details are given below.

The main aspect to observe for all the structures when compared to the respective ground-state geometry is the strong increase in the phenyl bond lengths at the substituent-bearing carbons; namely, for the solvated system we obtain +0.042 and +0.014 Å for RC_1C_2 and +0.026 and +0.048 for $R_{C_3C_4}$, in the

TABLE 2: TDA/6-31G(d) Optimized Geometries for the Lowest Excited State of DMABN In Vacuo and in Acetonitrile Solution[a]

	acetonitrile		vacuum
	planar	twisted	twisted
$R_{N_8C_7}$	1.1579	1.1479	1.1429
$R_{C_7C_1}$	1.3937	1.4098	1.4209
$R_{C_1C_2}$	1.4510	1.4236	1.4149
$R_{C_2C_3}$	1.3496	1.3502	1.3528
$R_{C_3C_4}$	1.4493	1.4708	1.4648
$R_{C_4C_9}$	1.3553	1.3353	1.3416
$R_{N_9C_{10}}$	1.4513	1.4607	1.4553
$\angle C_2C_1C_7$	120.9	121.0	121.1
$\angle C_3C_4C_9$	121.5	116.6	121.2
$\angle C_{10}N_9C_{11}$	118.6	121.2	119.1

[a] The geometrical parameters refer to planar (0° twisting angle) and twisted (90° twisting angle) conformations; for the isolated system, only the twisted geometry was considered. Bond lengths are in Å, and angles are in degrees.

planar and the twisted cases, respectively. On the contrary, the bond lengths of the carbons between (here represented by R) become shorter (around −0.03 Å for all structures). In both the twisted structures, a significant decrease with respect to the corresponding ground-state value of the amino ring bond is observed; this can be explained in terms of the increase of the decoupling of the amino group from the π-system in the twisted excited states.

The analysis of these geometrical data becomes clearer when accompanied by the exploration of excited-state potential energy surfaces as obtained from the related excitation energies; here, however, some preliminary comments are required. The TDA theory has proven in the past to deliver accurate geometries for a number of different molecules; however, it is also known that this method is usually not adequate for computing excitation energies due to the neglect of dynamical electron correlation. Concerning DMABN, it has been found,[25,31] and our calculations have confirmed, such findings, that TDA theory gives an incorrect ordering of the first excited states for the isolated molecule, lowering the L_a-like CT state below the L_b-like LE for all twisting angles. More accurate QM calculations,[19,23] on the contrary, show that, at planar and near planar structures, the less dipolar LE state is preferentially stabilized.

The correct order can be recovered in the framework of linear response theories if we pass to the DFT level and exploit the previously recalled TDDFT method;[27] it thus becomes interesting to test here, for the first time, the behavior of TDDFT calculations in the presence of solvent effects. Unfortunately, the extension of the PCM solvation method to TDDFT analytical derivatives to get optimized geometries in solution is not yet available, so the comparison between the two methods will be limited to single point calculations.

In Figures 1−2 we report the energy curves for the ground and the first two singlet excited states both in vacuo and in acetonitrile, as obtained through TDDFT calculations. These curves were obtained by keeping the geometry of the ground state and changing the twisting angle between the amino group and the benzene ring from 0° (the planar structure) to 90° (the twisted structure).

The main difference between isolated and solvated systems is the absence of any crossing between the excited states; already at 0° twisting angle, the lowest excited state of DMABN in acetonitrile is easily identified, with the CT state being characterized by both a long-axis transition moment and a large oscillator strength. This is in contrast with the isolated molecule, in which the first excited state (the previously quoted

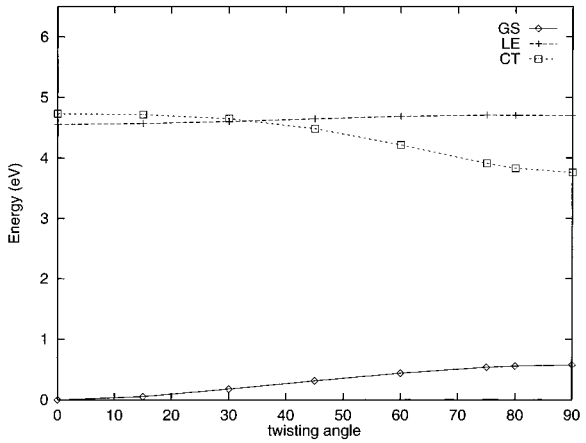

Figure 1. TDDFT potential energy curves (energy relative to the minimum of the ground state) of the ground and first two singlet excited states of DMABN in vacuo as a function of the dimethylamino twisting angle.

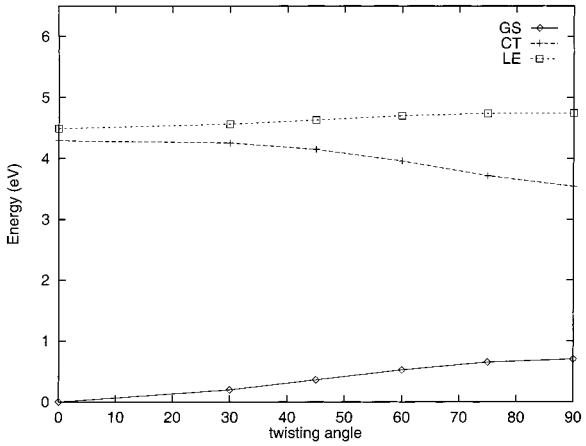

Figure 2. TDDFT potential energy curves (energy relative to the minimum of the ground state) of the ground and first two singlet excited states of DMABN in acetonitrile solution as a function of the dimethylamino twisting angle.

LE) presents a short-axis transition moment and almost zero oscillatory strength.

Increasing the twisting angle in both the isolated and the solvated systems presents the same order of the states. Comparisons between TDDFT curves of Figure 2 and TDA geometry optimizations show that, in the case of the solvated system, TDDFT gives the same description of TDA, contrary to what it is found in vacuo; this puts enough confidence in the previous geometrical analysis, confirming the ability of the solvation model and of its extension to TDA level, to correctly describe the action of a polar solvent in stabilizing the CT state, in agreement with experimental evidence.

The solvent-induced changes in the excited-state order described by TDDFT calculations can be better explained in terms of dipole moments and population analysis. It has been proved that excited-state dipoles and properties are better computed with a relaxed density matrix and not the simple one-particle density matrix (1PDM). The evaluation of the relaxed density requires a CPHF-like derivative procedure not yet available at the TDDFT level for PCM solvated systems; thus, to evaluate excited-state properties, TDA calculations have to be exploited (see eqs 18−20).

The computed dipoles, group charges, and oscillator strengths for both the ground and lowest excited states of the solvated

TABLE 3: GS and Lowest Excited-State Dipoles (debye) and Group Charges (au) of DMABN at the Planar and Twisted Conformations in Acetonitrile Solution and at the Twisted Structure In Vacuo[a]

	acetonitrile				vacuum	
	planar		twisted		twisted	
	GS	exc	GS	exc	GS	exc
μ	10.1271	13.0671	6.9412	17.0420	5.4215	13.7120
NMe_2	−0.0695	−0.0340	−0.1651	0.2886	−0.1798	0.2645
Bz	0.4018	0.3896	0.4562	0.0624	0.4251	0.0071
CN	−0.3323	−0.3556	−0.2911	−0.3511	−0.2452	−0.2736
f		1.0419		0.0587		0.0000

[a] For excited states, oscillator strengths are also reported.

system (at 0° and 90° twisting angles) are reported in Table 3. Once again, for the twisted structure we also report the parallel values obtained in vacuo. Excited-state geometries are those reported in Table 2 (which have been optimized at the TDA level), whereas for the ground state, the B3LYP geometry of Table 1 was used (twisted GS geometry were obtained by just rotating the amino group 90°, keeping frozen all the other parameters).

From the results of Table 3, the nature of the solvent effects is evident; the strongly dipolar nature of the excited state, that previously identified as the CT state, is the origin of very effective interactions with the polar solvent, which lower the energy of this state with respect to the others at all twisting angles, as shown in Figure 2. Inspection of the computed group charges (obtained by summing up all the atomic Mulliken charges in each different moiety of the molecular system) illustrates how this charge transfer process occurs. As shown by the significant increase in the excited-state dipole and the parallel decrease in the amino group charge, there is some charge transfer already in the planar conformation, but this is considerably enhanced by the twisting; at 90° the charge on the amino group in the excited state has increased by about +0.45e with respect to the GS whereas a net decrease of −0.39e is found on the benzene ring. The analysis of data obtained for the twisted excited state in vacuo shows a by far weaker charge-transfer character of this state with respect to the parallel one in solution; both dipole and group charge values are intermediate between those of the planar and the twisted solvated systems.

This feature can be related to the different order in the excited states observed in vacuo and in solution. The partial CT nature of the excited state at the planar conformation is largely favored in a polar solvent because it leads to a net increase in the dipole with respect to the ground state and thus to a more stabilized system. The final result is a solvent-induced enhancement of this charge-transfer character, leading to a solvated planar state that presents characteristics very similar to those of the twisted state in vacuo even if a complete CT process is expected only for the latter.

This analysis can be repeated in terms of orbital excitations. In the planar conformation, the solvated CT state is mainly described by the single excitation $\pi \rightarrow \pi^*$ (HOMO → LUMO), where the contribution of the N lone pair is made through the delocalized nature of the HOMO and LUMO orbitals over the benzene plane. At the twisted geometry, the state is also characterized by a singly excited configuration but, this time, from the lone-pair (n) orbital to the LUMO (π^*) orbital, with the latter now completely localized to the benzonitrile moiety. This change in the nature of the CT state is reflected by the values of the oscillatory strength; from the large value characterizing the planar structure, it decreases almost to zero for completely decoupled subunits, thus indicating a transformation from the allowed $\pi \rightarrow \pi^*$ to the forbidden $n \rightarrow \pi^*$ transition.

Conclusions

We have developed and implemented the theory needed to obtain analytical derivatives of the excited-state energy surfaces of molecular systems in solution at the CI-singles level. In particular, solvent effects are included in both the evaluation of the relaxed density and in the computation of the energy gradients, without any approximation or neglect of terms. As remarked in the Introduction, the only assumption we exploit is that the poles of the linear response function also represent proper excitation energies for condensed systems. The trial calculations on DMABN demonstrate that this approach is practical and the results are reasonable. In particular, they show that even this simplified CI scheme, when coupled with an accurate solvation model, can predict the correct behavior of complex processes involving excited states of very different natures. In addition, the introduction of solvent terms, not altering the efficiency of the original method formulated for isolated systems, preserves the important characteristic of the TDA approximation of being easily applicable to large molecular systems.

However, we have also shown that a more refined description of the excited states requires more accurate methods. A surely promising approach is the TDDFT, which has already demonstrated very good performances in describing potential energy surfaces (and the related excitation energies) of excited states for many isolated systems. Here, we have found that the same accuracy can also be achieved for solvated systems; we are thus confident that solvent terms, when treated within the PCM model, still preserve the same good behavior in the calculation of energy derivatives and related properties. Indeed, the theory presented here can be extended to TDDFT without any specific modifications concerning the solvation component. Numerical results on this extension will be presented soon.

Acknowledgment. One of the authors (R.C.) acknowledges the Italian CNR (Consiglio Nazionale delle Ricerche: Progetto Finalizzato "Materiali Speciali per Tecnologie Avanzate II") and MURST (Ministero dell'Universitá e della Ricerca Scientifica e Tecnologica: "Cofinanziamento 97") for financial support.

References and Notes

(1) Foresman, J. B.; Head-Gordon, M.; Pople, J. A.; Frisch, M. J. *J. Phys. Chem.* **1992**, *96*, 135.

(2) (a) Ooshika, Y. *J. Phys. Soc. Jpn*. **1954**, *9*, 594. (b) Marcus, R. J. *Chem. Phys*. **1956**, *24*, 966. (c) McRae, E. G. *J. Phys. Chem*. **1957**, *61*, 562. (d) Basu, S. *Adv. Quantum. Chem*. **1964**, *1*, 145. (e) Levich, V. G. *Adv. Electrochem. Eng*. **1966**, *4*, 249. (f) Kim, H. J.; Hynes, J. T. *J. Chem. Phys*. **1990**, *93*, 5194, 5211. (g) Berezhkosvskii, A. M. *Chem. Phys*. **1992**, *164*, 331. (h) Basilevski, M. V.; Chudinov, G. E. *Chem. Phys*. **1990**, *144*, 155. (i) Aguilar, M. A.; Olivares del Valle, F. J.; Tomasi, J. *J. Chem. Phys*. **1993**, *98*, 7375. (j) Cammi, R.; Tomasi, J. *Quantum Chemistry Symposium, Int. J. Quantum Chem*. **1995**, *29*, 465.

(3) Cammi, R.; Mennucci, B. *J. Chem. Phys*. **1999**, *110*, 9877.

(4) (a) Jonsson, D.; Norman, P.; Ågren, H.; Luo, Y.; Sylvester-Hvid, K. O.; Mikkelsen, K. V. *J. Chem. Phys*. **1998**, *109*, 6351. (b) Mikkelsen, K. V.; Luo, Y.; Ågren, H.; Jorgensen, P. J. *J. Chem. Phys*. **1994**, *100*, 8240.

(5) (a) Miertus, S.; Scrocco, E.; Tomasi, J. *Chem. Phys*. **1981**, *55*, 117. (b) Cammi, R.; Tomasi, J. *J. Comput. Chem*. **1995**, *16*, 1449.

(6) (a) Cancès, E.; Mennucci, B. *J. Math. Chem*. **1998**, *23*, 309. (b) Cancès, E.; Mennucci, B.; Tomasi, J. *J. Chem. Phys*. **1997**, *107*, 3032. (c) Mennucci, B.; Cancès, E.; Tomasi, J. *J. Phys. Chem. B* **1997**, *101*, 10506.

(7) Ortiz, J. V. *J. Chem. Phys*. **1994**, *101*, 6743.

(8) Casida, M. E. *Recent Advances in Density Fuctional Methods*; Chong, D. P., Ed.; World Scientific: Singapore, 1995, Vol. 1. (b) Casida, M. E. *Recent Developments and Applications of Modern Density Functional Theory, Theoretical and Computational Chemistry*; Seminario, J. M., Ed.; Elsevier: Amsterdam, 1996; Vol. 4.

(9) Stratmann, R. E.; Scuseria, G.; Frisch, M. J. *J. Chem. Phys*. **1998**, *109*, 8218.

(10) Bauernschmitt, R.; Ahlrichs, R. *Chem. Phys. Lett*. **1996**, *256*, 454.

(11) Tozer, D. J.; Handy, N. C. *J. Chem. Phys*. **1998**, *109*, 10180.

(12) Hirata, S.; Head-Gordon, M. *Chem. Phys. Lett*. **1999**, *314*, 291.

(13) (a) Van Caillie, C.; Amos, R. D. *Chem. Phys. Lett*. **1999**, *308*, 249. (b) Van Caillie, C.; Amos, R. D. *Chem. Phys. Lett*. **2000**, *317*, 159.

(14) McWeeny, R. *Methods of Molecular Quantum Mechanics*, 2nd ed.; Academic Press: London, 1992.

(15) Cammi, R.; Cossi, M.; Mennucci, B.; Tomasi, J. *J. Chem. Phys*. **1996**, *105*, 10556.

(16) Cammi, R.; Mennucci, B.; Tomasi, J. *J. Phys. Chem. A* **1999**, *103*, 9100.

(17) Handy, N. C.; Schaefer, H. F., III *J. Chem. Phys*. **1984**, *81*, 5031.

(18) (a) Cancès, E.; Mennucci, B. *J. Chem. Phys*. **1998**, *109*, 249. (b) Cancès, E.; Mennucci, B.; Tomasi, J. *J. Chem. Phys*. **1998**, *109*, 260.

(19) Mennucci, B.; Toniolo, A.; Tomasi, J. In preparation.

(20) Lippert, E.; Lüder, W.; Moll, F.; Nägele, W.; Boos, H.; Prigge, H.; Seibold-Blankestein, I. *Angew. Chem*. **1961**, *73*, 695.

(21) (a) Rotkiewicz, K.; Grellmann, K. H.; Grabowski, Z. R. *Chem. Phys. Lett*. **1973**, *19*, 315. (b) Siemiarczuk, A.; Grabowski, Z. R.; Krowczynski, A.; Asher, M.; Ottolenghi, M. *Chem. Phys. Lett*. **1977**, *51*, 315.

(22) Schuddeboom, W.; Jonker, S. A.; Wartman, J. M.; Leinhos, U.; Kühnle, W.; Zachariasse, K. A. *J. Phys. Chem*. **1992**, *96*, 10809.

(23) Serrano-Andrés, L.; Merchán, M.; Roos, B. O.; Lindh, R. *J. Am. Chem. Soc*. **1995**, *117*, 3189.

(24) Broo, A.; Zerner, M. C. *Chem. Phys. Lett*. **1994**, *227*, 551.

(25) (a) Scholes, G. D.; Phillips, D.; Gould, I. R. *Chem. Phys. Lett*. **1997**, *266*, 521. (b) Scholes, G. D.; Gould, I. R.; Parker, A. W.; Phillips, D. *Chem. Phys*. **1998**, *234*, 21.

(26) Frisch, M. J.; Trucks, G. W.; Schlegel, H. B.; Scuseria, G. E.; Robb, M. A.; Cheeseman, J. R.; Zakrzewski, V. G.; Montgomery, J. A., Jr.; Stratmann, R. E.; Burant, J. C.; Dapprich, S.; Millam, J. M.; Daniels, A. D.; Kudin, K. N.; Strain, M. C.; Farkas, O.; Tomasi, J.; Barone, V.; Cossi, M.; Cammi, R.; Mennucci, B.; Pomelli, C.; Adamo, C.; Clifford, C. S.; Ochterski, J.; Petersson, G. A.; Ayala, P. Y.; Cui, Q.; Morokuma, K.; Malick, D. K.; Rabuck, A. D.; Raghavachari, K.; Foresman, J. B.; Cioslowski, J.; Ortiz, J. V.; Stefanov, B. B.; Liu, G.; Liashenko, C. A.; Piskorz, P.; Komaromi, I.; Gomperts, R.; Martin, R. L.; Fox, D. J.; Keith, T.; Al-Laham, M. A.; Peng, C. Y.; Nanayakkara, A.; Gonzalez, C.; Challacombe, M.; Gill, P. M. W.; Johnson, B.; Chen, W.; Wong, M. W.; Andres, J. L.; Head-Gordon, M.; Replogle, E. S.; Pople J. A. *Gaussian 99*, Development Version, Revision A.10; Gaussian, Inc.: Pittsburgh, 1999.

(27) Parusel, A. B. J.; Köhler, G.; Grimme, S. *J. Phys. Chem. A* **1998**, *102*, 6297.

(28) (a) Mikkelsen, K. V.; Cesar, A.; Ågren, H.; Jensen, H. J. A. *J. Chem. Phys*. **1995**, *103*, 9010. (b) Mikkelsen, K. V.; Sylvester-Hvid, K. O. *J. Phys. Chem*. **1996**, *100*, 9116. (c) Mennucci, B.; Cammi, R.; Tomasi, J. *J. Chem. Phys*. **1998**, *109*, 2798. (d) Mennucci, B.; Toniolo, A.; Cappelli, C. *J. Chem. Phys*. **1999**, *110*, 6858.

(29) Lommatzsch, U.; Brutschy, B. *Chem. Phys*. **1998**, *234*, 35.

(30) Heine, A.; Herbst-Irmer, R.; Stalke, D.; Kühnle, W.; Zachariasse, K. A. *Acta Crystallogr. B* **1994**, *50*, 363.

(31) (a) Sobolewski, A. L.; Sudholt, W.; Domcke, W. *J. Phys. Chem. A* **1998**, *102*, 2716. (b) Sudholt, W.; Sobolewski, A. L.; Domcke, W. *Chem. Phys*. **1999**, *240*, 9.